



t

Final Report

g-2 tracker characterization

Eleonora Rossi

J-1 Summer Student from

Università degli Studi di Roma Tre

Supervisor: **Brendan Casey**

Contents

1	The new g-2 experiment at Fermilab	2
1.1	What is physical significance of g factor?	2
1.2	What about muons?	3
1.3	How to measure g? The g-2 experiment	4
1.4	Tracking detectors	5
1.4.1	The straw tracker	6
2	Data analysis: characterization of the performance of the straw detector	9
2.1	Testing different gas mixtures with different sources: plateau curves	10
2.2	Estimation of S/N and gain	11
2.3	Test beam data: estimation of S/N	13
2.4	Test beam data: crosstalks	15
2.5	Test beam simulation	17
2.6	Detector efficiency	18
2.6.1	Comparison between simulation and real data with 4 layers	18
2.6.2	Comparison between simulation and real data with just 3 layers	20

Introduction

Precise measurements of fundamental quantities have played a key role in the development of Theoretical Physics models such as the Standard Model¹. Though this model describes so many physical phenomena and has demonstrated huge successes in providing experimental predictions, it is necessarily incomplete because it does leave something unexplained.

The $g-2$ factor represents an important test of the Standard Model because of a long standing discrepancy, that is more than three standard deviations, between SM predictions and Brookhaven muon experiment values.

The new $g-2$ experiment at Fermilab plans to improve the experimental uncertainties by a factor of 4 and it is expected that there will be a significant reduction in the uncertainty of the SM predictions.

A brief description of experimental apparatus and main detectors will be reported.

The main task of my job has been the characterization of the straw tracker detector; in other words I tried to find out which kind of gas mixture could be the most suitable and the most efficient for the experiment (ArCO₂ or ArEt) and, in the meantime, I tried to understand if the detector has worked properly.

In my analysis I used measurements taken at the Test Beam Facility (August 2015) and data taken from the Tracker Test Beam T1042 (June 2015).

¹SM

Chapter 1

The new g-2 experiment at Fermilab

1.1 What is physical significance of g factor?

Any charged particle, whose spin is equal to $\frac{1}{2}$, has an intrinsic magnetic moment $\vec{\mu}$ that is aligned with its spin vector \vec{s} :

$$\vec{\mu} = g \frac{q}{2m} \vec{s} \quad (1.1)$$

where $q(m)$ is the particle's charge and g is the gyromagnetic factor.

As well as we can see from Equation (1.1), the g -factor dictates the relationship between momentum and spin, telling us something fundamental about the particle itself (and those interacting with it).

In a classical system $g = 1$; elementary particles such as electrons, as predicted by Dirac, should have $g = 2$.

A large discrepancy between the theoretical prediction and a measurement of the hydrogen hyperfine structure prompted work by Schwinger that ultimately resolved this disagreement and initiated the field of QED.

In fact, for particles such as the electron, the classical result differs from the observed value by a small fraction of a percent.

The difference is the anomalous magnetic moment, denoted a and defined as:

$$a = \frac{g - 2}{2} \quad (1.2)$$

The one-loop contribution to the anomalous magnetic moment, that corresponds to the first and largest quantum mechanical correction, is found by calculating the vertex function shown in *Figure 1.1 b*).

The calculation is relatively straightforward and the *one - loop* result is:

$$a = \frac{\alpha}{2\pi} \approx 0.0011614 \quad (1.3)$$

where α is the fine structure constant.

This result was first found by Julian Schwinger in 1948 and is engraved on his tombstone.

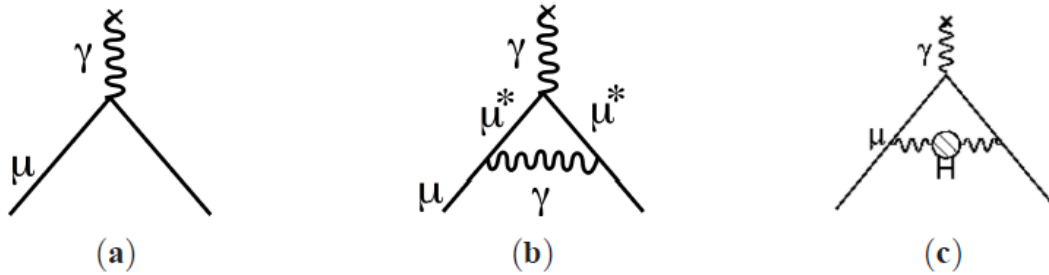


Figure 1.1: Feynman diagrams for $g=2$ (a), the Schwinger term (b), and the first-order vacuum polarization contribution (c)

1.2 What about muons?

“Muons are special. They are light enough to be produced copiously, yet heavy enough that we can use them experimentally to uniquely probe the accuracy of the Standard Model.” Chris Polly, Particle Physicist at Fermilab

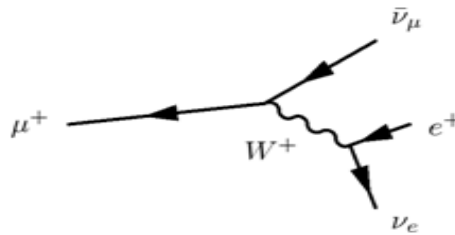


Figure 1.2: Muon decay

The muon is an elementary particle similar to the electron with a mass that is about 200 times the mass of the electron; the word “similar” means that they have similar interaction types.

Muons are produced from the interactions between an energetic proton beam and a light-element target. The proton collisions produce pions, which decay into muons. The muon beam produced can be 100% spin polarised, i.e. all the muon spins are pointing in the same direction. This is a key feature of the muon technique, as it is what happens to the muon polarisation which we observe in muon experiments.

After an average lifetime of $2.2 \mu s$, a lifetime long enough to guarantee an easy way to make sample production, each muon decays and emits a positron. The decay positrons are preferentially emitted in the muon spin direction, they are detected, and tell us about how the muons’ spins were behaving in the sample.

The anomalous magnetic moment of the muon is calculated in a similar way; its measurement provides a precision test of the Standard Model. The interactions between virtual particles and real particles perturb the gyromagnetic factor g at the 0.1% level for muons, as well as for electrons: these radiative corrections are applied due to the fact that space is never empty but it has virtual particles pop in and out within short period. The perturbation is dominantly due to electromagnetic single photon exchange but the exact value

is sensitive to all such allowed interactions.

The prediction for the value of the muon anomalous magnetic moment includes three parts:

$$a_{\mu}^{\text{SM}} = a_{\mu}^{\text{QED}} + a_{\mu}^{\text{EW}} + a_{\mu}^{\text{Had}} + \dots \quad (1.4)$$

The muon anomaly provides a unique window to search for Physics beyond the Standard Model.¹ Perhaps the ultimate value of an improved limit on a_{μ} will come from its ability to constrain the models that have not yet been invented.[1]

1.3 How to measure g? The g-2 experiment

In 2009, the New Muon g-2 Collaboration proposed a new experiment for Fermilab that promises to reduce² the experimental uncertainty on the muon anomalous magnetic moment by a factor of 4, to a precision of $\delta a_{\mu} = 16 \times 10^{-11}$. This is an impressive step forward, requiring more than 20 times the statistics acquired in three running periods at Brookhaven.

Custom short “bunches” of protons will be formed in the Recycler and delivered one at time to the existing antiproton target. A 3.1 GeV positive pion beam will be directed out of the target and along a 290 m beamline. Most of the pions will decay along the way and forward-going, highly polarised, muons will be captured in the line. The muons are directed around the antiproton accumulator complex and then back toward the target region along a parallel transfer line. The resulting pure muon beam is injected in the storage ring. The relocated storage ring³ will be placed in a new, custom building near the target region and the final beam elements direct muons up to the surface and into the ring, where they are kicked on a orbit. [2]

Under the influence of a magnetic field \vec{B} , a muon will exhibit two important behaviors.

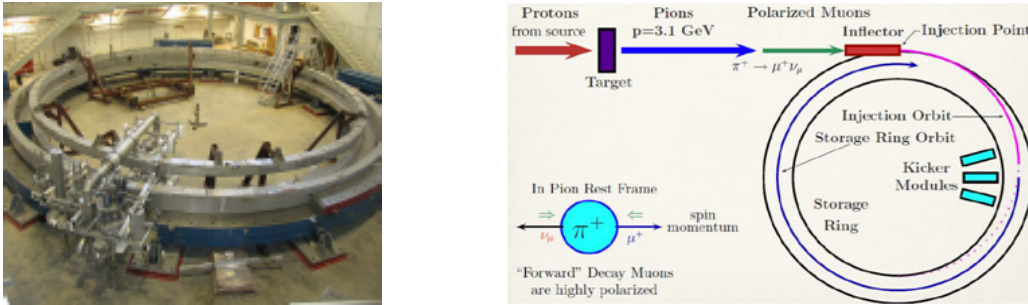


Figure 1.3: The new experiment: g-2 ring and g-2 project

Kinematically, its momentum will rotate ($\frac{d\vec{p}}{dt} = e\vec{v} \times \vec{B}$) with a frequency given by:

$$\omega_c = \frac{eB}{\gamma mc} \quad (1.5)$$

¹The more than 2000 citations to the major E821 (Brookhaven experiment) papers demonstrates this role

²in comparison with the Brookhaven experiment

³from Brookhaven

where ω_c is the cyclotronic frequency.

Continual momentum rotation allows for muon storage.

The second important behavior is the Larmor precession of its spin vector due to torque provided by the magnetic field ($\frac{d\vec{s}}{dt} = \vec{\mu} \times \vec{B}$) with a frequency given by:

$$\omega_s = \frac{g_\mu eB}{2mc} + (1 - \gamma) \frac{eB}{\gamma mc} \quad (1.6)$$

where ω_s is the spin rotation frequency.

Assuming the velocity is entirely perpendicular to the magnetic field, the measurable difference of the two quantities ω_s and ω_c is directly sensitive to the muon anomaly a_μ : [3]

$$\omega_a = \omega_s - \omega_c = a_\mu \frac{qB}{m} \quad (1.7)$$

The pure ($V - A$) three-body weak decay of the muon, $\mu^- \rightarrow e^- + \nu_\mu + \bar{\nu}_e$ or $\mu^+ \rightarrow e^+ + \bar{\nu}_\mu + \nu_e$, is “self-analyzing”, that is, the parity-violating correlation between the directions in the muon rest frame (MRF) of the decay electron and the muon spin can provide information on the muon spin orientation at the time of the decay. [1]

a_μ uncertainty source	BNL (ppb) [1]	FNAL goal (ppb) [9]
ω_a statistics	480	100
ω_a systematics	180	70
ω_p systematics	170	70
Total	540	140

Figure 1.4: Summary of experimental uncertainty for the BNL (Brookhaven) muon $g - 2$ measurement and projections for the new experiment at Fermilab

1.4 Tracking detectors

The new experiment will require upgrades of detectors, electronics and data acquisition equipment to handle the much higher data volumes and slightly higher instantaneous rates.

The primary physics goal of the tracking detectors is to measure the muon beam profile at multiple locations around the ring as a function of time throughout the muon fill. This information will be used to determine several parameters associated with the dynamics of the stored muon beam.

The secondary physics goal of the tracking detectors involves understanding systematic uncertainties associated with the muon precession frequency measurement derived from calorimeter data. In particular, the tracking system will isolate time windows that have multiple positrons hitting the calorimeter within a short time period and will provide an independent measurement of the momentum of the incident particle.

The tertiary physics goal of the tracking detectors is to determine if there is any tilt in

the muon precession plane away from the vertical orientation. [1]

In-vacuum straw drift tubes will be used to measure the characteristics of the muon beam, and provide data for an improved muon electric dipole moment measurement. [4]

1.4.1 The straw tracker

The preliminary design is an array of straw tubes with alternating planes oriented 7.5° from the vertical direction.

We refer to the plane with negative slope as the U plane and the plane with the positive slope as the V plane with respect to the radial-vertical plane.

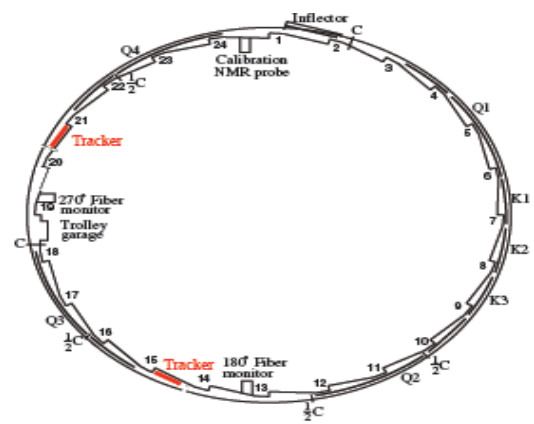
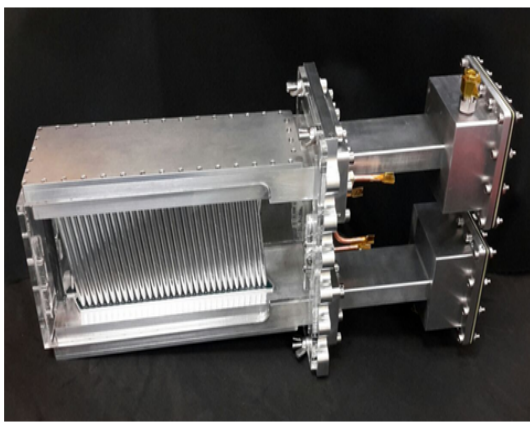


Figure 1.5: A tracking module and its position

The required number of planes, along with the need to minimize multiple scattering lead to the choice of a gas based detector. The requirement to place the detectors in the vacuum leads to the choice of straws since the circular geometry can hold the differential pressure with minimal wall thickness. [1]

Straw or tube chambers are basically proportional chambers constructed with a single anode wire centered in an aluminized plastic tube forming the grounded cathode.

The advantages of a straw chamber when compared to multiwire chambers are: [5]

- the straw chamber is inexpensive, robust and relatively simple to construct;
- the damage and possible down time caused by wire breakage is minimal since the broken wire is isolated in the tube cell and will only need to be disconnected;
- the effect of signal cross talk are minimized as the straw cathode provides a complete ground shield between nearby wires;
- the problems of electrostatic alignment distortions are minimal when the anode is kept reasonably centered in the straw.

The main disadvantage is the amount of material the straw introduces into the chamber. This causes more multiple scattering and reduces the momentum resolution.

In order to minimize multiple scattering of muons and positrons, g-2 muon storage volume, which lies within the 1.45 T magnetic field, is evacuated.

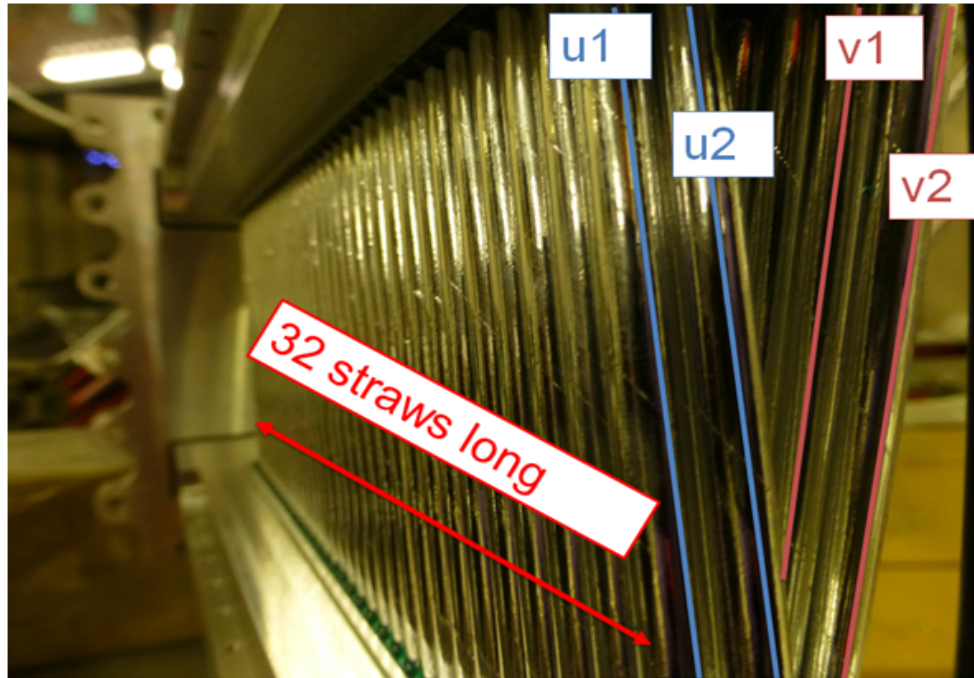


Figure 1.6: The straw tracker: overview

Gas distribution

The choice of the drift gas that has to fill the detector, between the wire and the walls of the straw, is guided by gain, efficiency, convenience and economic reasons.

The typical mixture is composed by a noble gas and a quencher.

Avalanche multiplication occurs in noble gases at much lower fields than in complex molecules: this is a consequence of the many non-ionizing energy dissipation modes available in polyatomic molecules. Therefore, convenience of operation suggests the use of a noble gas as the main component; addition of other components will of course slightly increase the threshold voltage.

The choice within the family of noble gases is then dictated by a high specific ionization; disregarding for economic reasons the expensive Xenon or Krypton, the choice naturally falls on Argon.

During the avalanche process, excited and ionized atoms are formed.

The excited noble gases can return to the ground state only through a radiative process, and the minimum energy of the emitted photon (11.6 eV for Argon) is well above the ionization potential of any metal constituting the cathode (7.7 eV for Copper). Photoelectrons can therefore be extracted from the cathode, and initiate a new avalanche very soon after the primary.

Argon ions, on the other hand, migrate to the cathode and are there neutralized extracting an electron; the balance of energy is either radiated as a photon, or by secondary

emission, i.e. extraction of another electron from the metal surface. Both processes result in a delayed spurious avalanche: even for moderate gains, the probability of the processes discussed is high enough to induce a permanent regime of discharge.

The large amount of non-radiative excited states (rotational and vibrational) allows the absorption of photons in a wide energy range: for methane, for example, absorption is very efficient in the range 7.9 to 14.5 eV, which covers the range of energy of photons emitted by argon. This is a common property of most organic compounds in the hydrocarbon and alcohol families, and of several inorganic compounds like freons, CO₂, BF₃, and others. The molecules dissipate the excess energy either by elastic collisions, or by dissociation into simpler radicals. [6]



Figure 1.7: The straws

Chapter 2

Data analysis: characterization of the performance of the straw detector

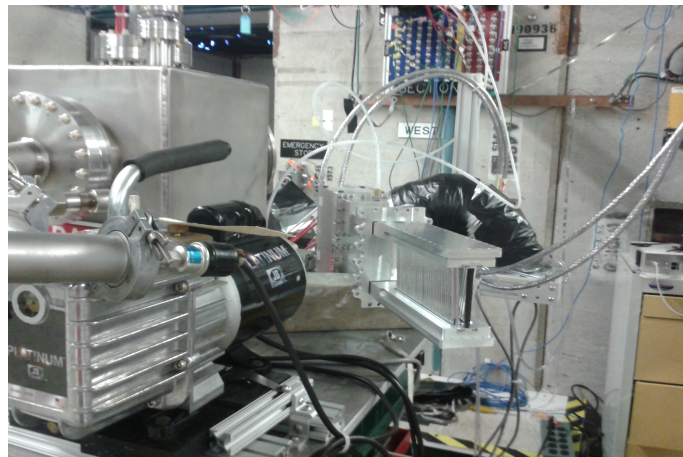


Figure 2.1: The experimental setup used for plateau and gain measurements

In order to characterize the performance of the detector and to understand if it was working properly, we tested two different gas mixtures, $ArCO_2$ and $ArEt$, with two different sources, ^{90}Sr and ^{55}Fe .

The use of these different sources led us to two different analysis: the study of the plateau curves and the study of the gain and of the ratio $\frac{S}{N}$.

The choice of the most suitable gas mixture goes through its main features :

- **ArEt:**
 - works better at high gain;
 - flammable.
- **ArCO₂:**
 - doesn't work at high gain;

- cheaper;
- not flammable.

2.1 Testing different gas mixtures with different sources: plateau curves

We illuminated the straws with a ^{90}Sr source; this source was weakly collimated so we were hitting several straws at once.

Looking at Figure 2.2, it is possible to see a breaking down point which constitutes a validation of ArCO_2 features: after this point we couldn't count anymore.

The higher rate in ArCO_2 may be because of the beginning of breakdown.

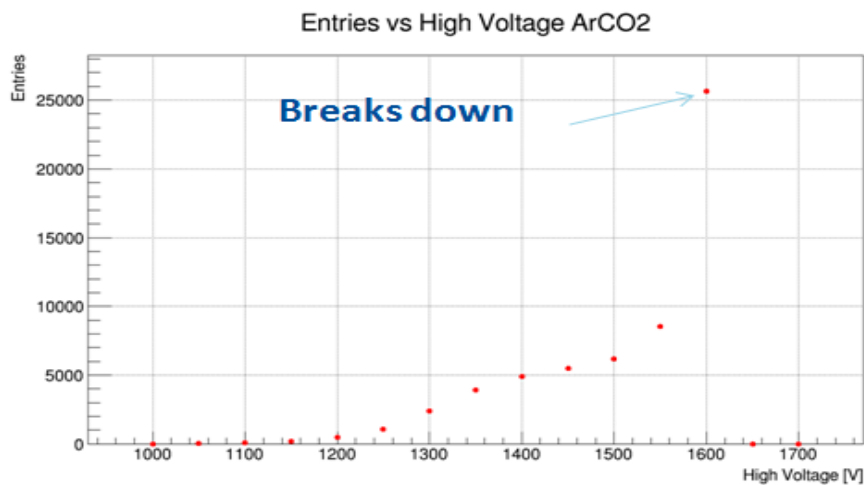


Figure 2.2: ArCO2 plateau curve

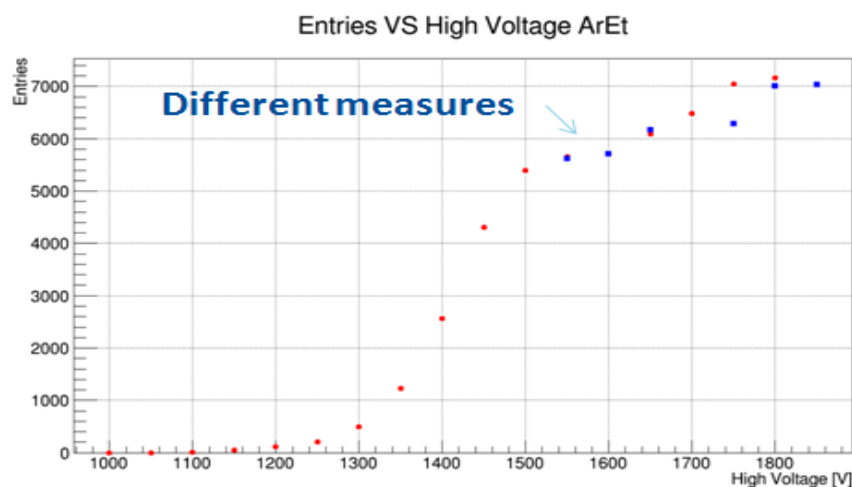


Figure 2.3: ArEt plateau curve

Regarding $ArEt^1$ we observed an unexpected behavior: there is no turn over at all. In order to understand these measurements, we repeated them from 1550 V to 1800 V obtaining same results.

Therefore this discrepancy could be an indication of saturation in the ASDQ.

It is better to underline that no timing information was used in making these plots so they indicate that the threshold was being crossed but not that the ASDQ output was reasonable.

2.2 Estimation of S/N and gain

The characterization of the performance of the straw tube detector goes through the estimation of the gain; in order to achieve this goal we illuminated the straws with a ^{55}Fe source; the gain is calculated through two steps:

- First step: determination of the threshold that corresponds to half of the rate using the intercept of the fitting line, a line that fits the “Entries VS Threshold” plot;
- Second step: determination of expected charges using the calibration curve (Figure 2.7) and the extrapolated thresholds (at 50%).

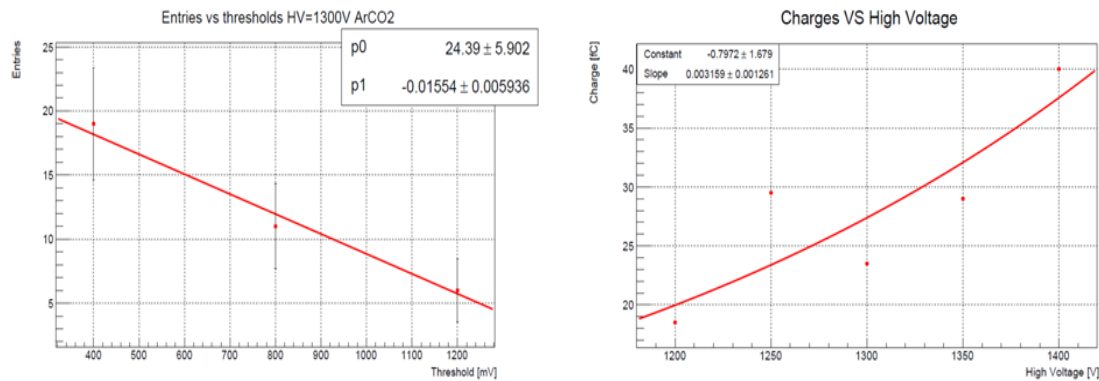


Figure 2.4: ArCO2 plots

$ArCO_2$ was tested only outside of the vacuum chamber.

Fitting the “Charge VS High Voltage” plot with an exponential curve, we estimated the expected charge for $HV = 1500 V$: $C = 51,6 fC$.

In the knowledge that the noise on the threshold is $N = 0,3 V$ and corresponds to a noise on the charge $N_c = 7 fC$, we calculated the ratio:²

$$\frac{S}{N} \approx 7,4$$

Ideally this ratio should be like 10 : 1, so a ratio that is higher than 7 : 1 looks pretty good.

¹Figure 2.3

²where S stands for signal and N stands for noise

ArEt was tested both in the vacuum chamber and outside of it.

Unlike *ArCO2*, it seemed that this gas mixture was not working really well. In fact, some data looked really bad and we couldn't understand the measurements we were taking. This behavior could be originated by the ^{55}Fe source not powerful enough or by the fact that we had few data with large errors.

If you look at Figure 2.6, it is clear that a fit with an increasing exponential curve should be really useless.

Therefore we decided to estimate just the charge value that corresponds to $HV = 1800\text{ V}$. In the knowledge that the noise on the threshold is $N = 0,3\text{ V}$ and corresponds to a noise on the charge $N_c = 7\text{ fC}$, considering $HV=1800\text{ V}$ outside and in the vacuum chamber, we estimated the ratios:

$$\frac{S}{N} \approx 3,3 \quad \text{outside} \quad \frac{S}{N} \approx 3,9 \quad \text{in the vacuum chamber}$$

Although it is good that the ratios outside and in the vacuum chamber are comparable, that means our detector is working properly in the vacuum and it is not damaged there, these ratios are supposed to be better. Ideally ratios should be like 10 : 1, so a ratio that is about 3 : 1 looks really bad. Furthermore *ArEt* ratio is supposed to be 10 times that of *ArCO2*: there was something wrong we didn't understand.

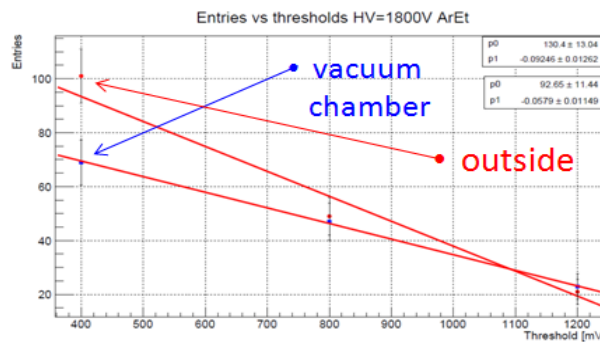


Figure 2.5: ArEt “Entries VS Threshold” plot

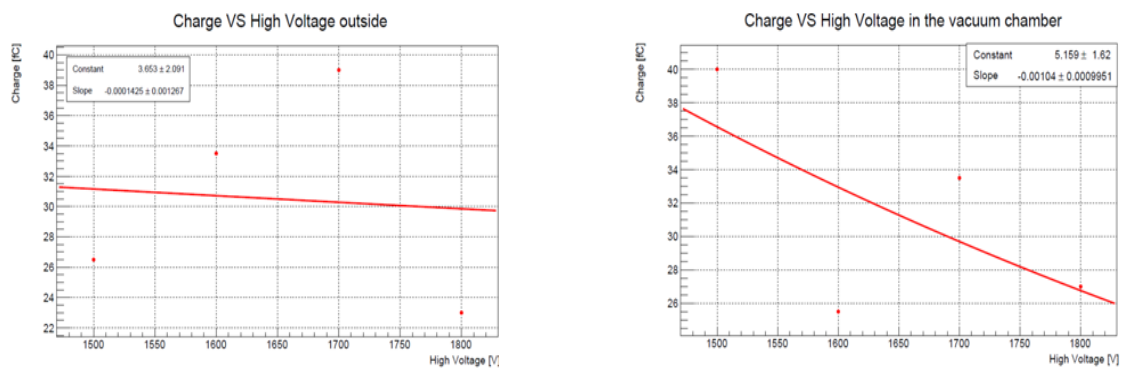


Figure 2.6: ArEt “Charge VS High Voltage” plots

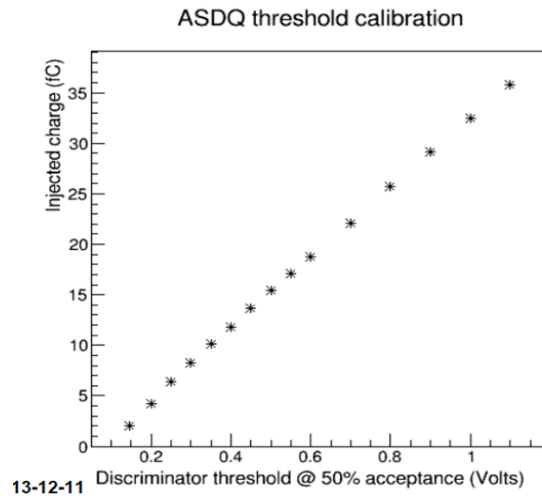


Figure 2.7: Calibration curve [7]

2.3 Test beam data: estimation of S/N

The characterization of the performance of the detector goes on with test beam data taken from the 120 GeV proton beam. The goal of this section is the estimation of the ratio S/N looking at time differences between hits: if hits are less than 500 ns apart, we are looking at the same particle: the detector is working properly.

Considering two layers means that we are just trying to understand if what is analysed is really the signal we are looking for.

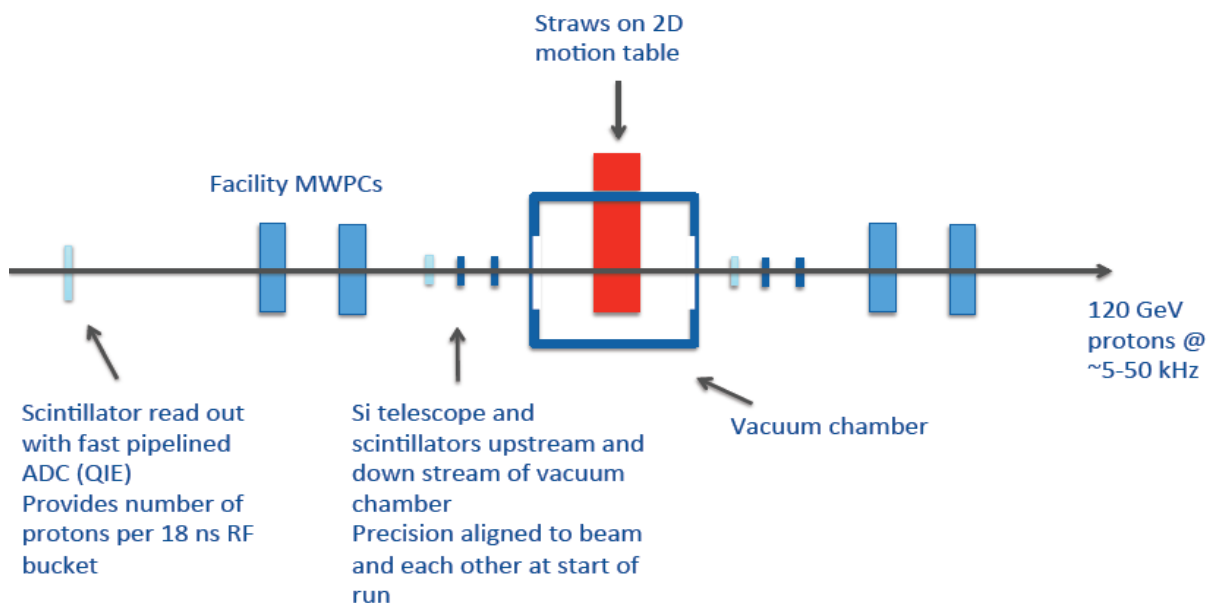


Figure 2.8: Beam test setup

A raw estimation of S/B^3 is given by *ArEt* 1700 V runs, combining a gaussian and a flat fit:

- run 401, $thr = 1000\text{ mV}$: $\frac{S}{B} \approx 5$;
- run 396, $thr = 700\text{ mV}$: $\frac{S}{B} \approx 3, 4$;
- run 395, $thr = 600\text{ mV}$: $\frac{S}{B} \approx 4, 6$;
- run 392, $thr = 500\text{ mV}$: $\frac{S}{B} \approx 4, 07$.

We should underline that, as well as you can see in ^{55}Fe ArEt data, these ratios are not really good in comparison with the ideal ratio, but this time we have to consider the fact that we are not using the maximum operating voltage.

If we look at 1800 V runs, we have many more entries and it is possible to fit every signal (time difference between $u1t$ and $u2t$) with a gaussian and a flat fit (Figure 2.9), in order to extrapolate fit parameters that are:

- **p0**: normalization of noise;
- **p1**: normalization of signal.

The calculation of $p1/p0$ is similar to the estimation of S/N .

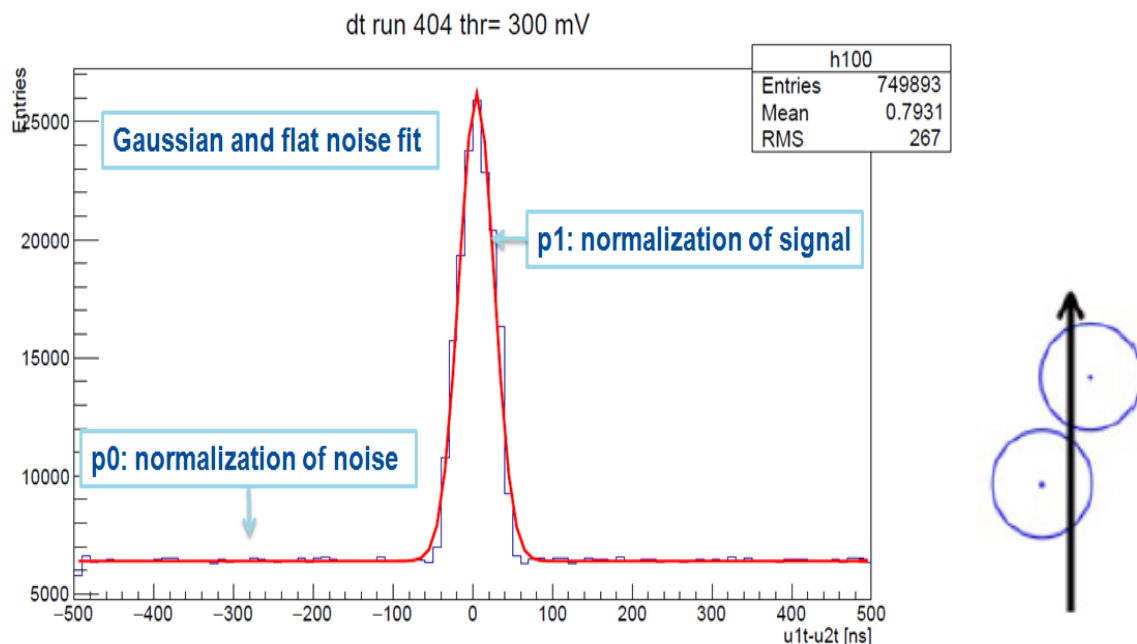


Figure 2.9: Example of a signal ($u1t-u2t$)

We are looking for a cut-threshold or a cut-value that could divide our signal from the noise.

³where S stands for signal and B stands for background

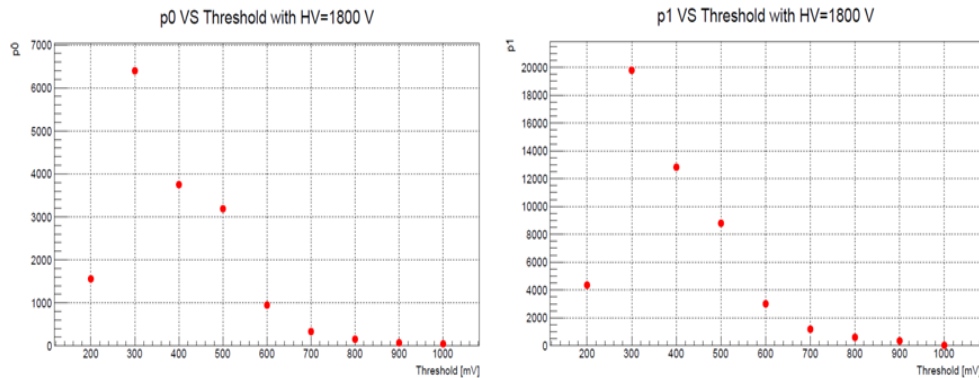


Figure 2.10: ArEt $HV = 1800 V$ $p0$ and $p1$

As well as you can see from Figure 2.10, we have two well-defined signals; but this is not true for the left side of Figure 2.11.

Therefore we tried to look for a normalization of our data which could be useful for us. Possible ways could be:

- normalization by the number of entries;
- normalization by the number of Protons per spill;
- normalization by the number of Packets in the event.

These normalizations turned out to be useless however, because we couldn't have the expected "well-defined shape" for every fit parameter at the same time.

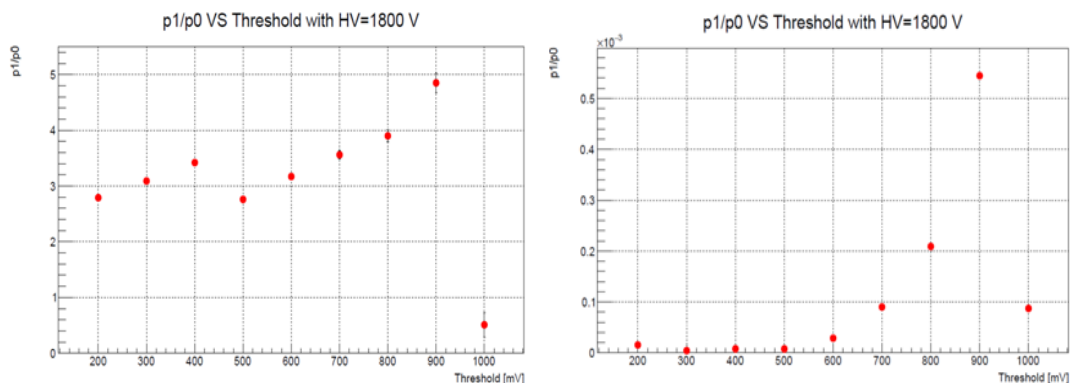


Figure 2.11: ArEt $HV = 1800 V$ $p1/p0$; on the right: normalization by the number of entries

2.4 Test beam data: crosstalks

The further step was the research of cross-talk between electronics channels, that is the cross-talk between near capacitors. [8]

We should analyse two cases:

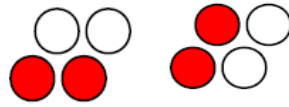


Figure 2.12: Cross-talk: on the left a); on the right b)

- adjacent straw of the same layer, a);
- adjacent straw of different layers, b).

It is really difficult to spot, because there are many similar signals; for example:

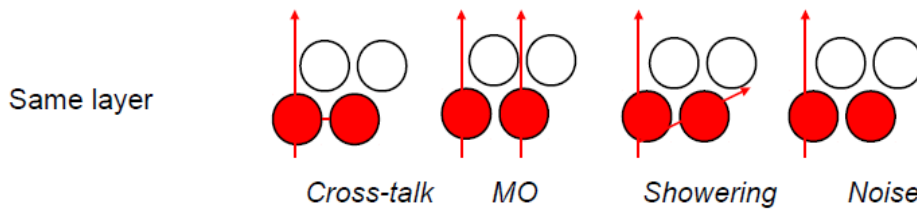


Figure 2.13: Examples of signals

We estimated fit parameters in two different configurations, that you can see on the right side of Figure 2.14 and 2.15 :

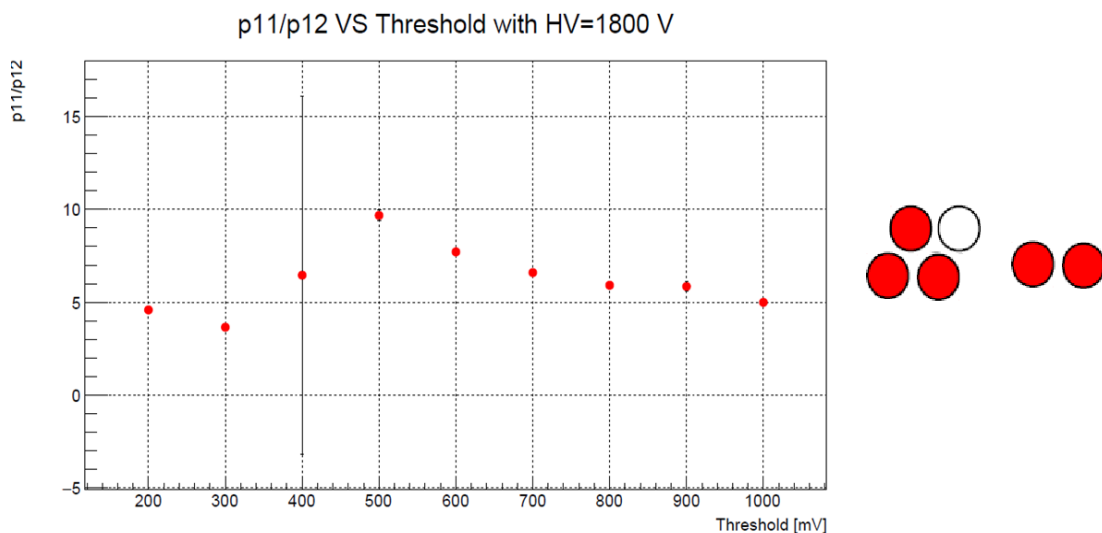


Figure 2.14: Cross-talks: parameters extrapolated by test beam data

Since these ratios are almost constant, within their uncertainty, we can conclude that, despite of a high occupancy in the beam, there is no real indication or evidence of cross-talk.

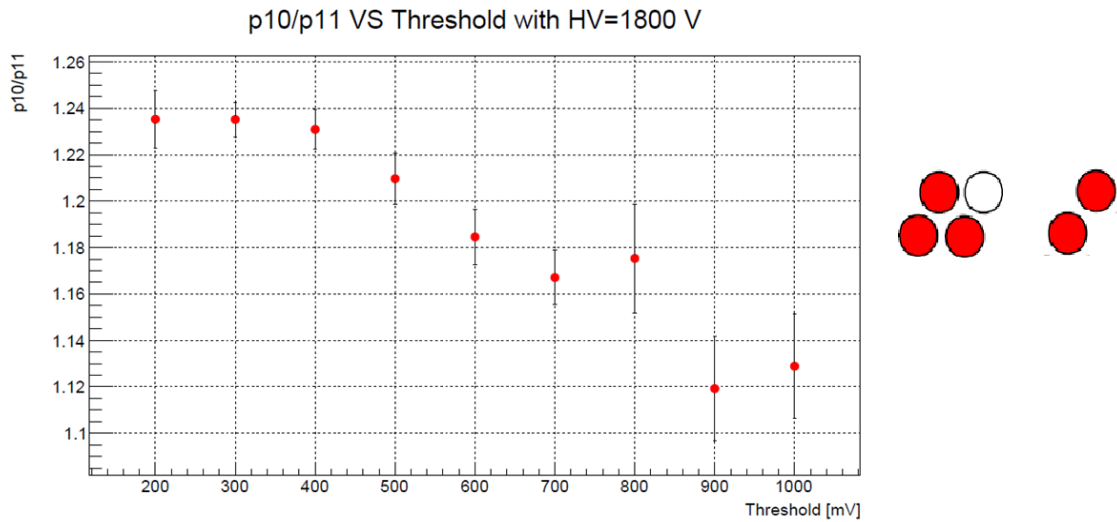


Figure 2.15: Cross-talks: parameters extrapolated by test beam data

Now, if we consider the normalizations of the noise, p_{10}/p_{11} , we have to note that the background goes down when we increase the threshold; so we can assert that we have noise in both straws but they are not correlated: this could be an indication of the fact that background is really background \rightarrow our data represent real particles.

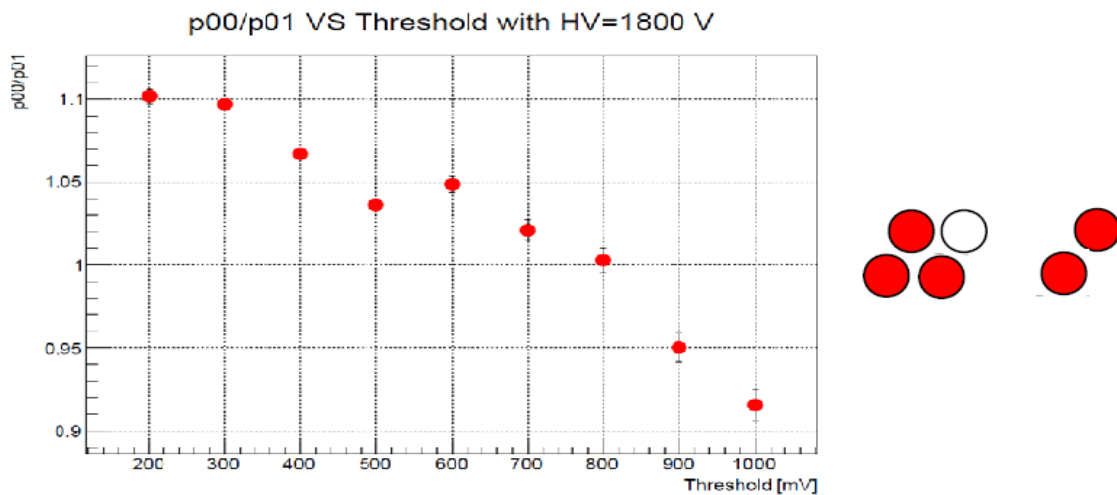


Figure 2.16: Cross-talks: parameters extrapolated by test beam data

2.5 Test beam simulation

In order to understand if our results were good, we used the tracker test beam simulation that is characterized by:

- aim to use same tools as for the real experiment;
- setting up analyses and reconstruction in art for use on both simulation and real data.

The straw track reconstruction consists of setting up a track finding algorithm for the tracking stations.

Eventually, Garfield straw simulations provide: [9]

- distributions and electron trajectories in the straws;
- induced currents on the wire;
- variety of gases/temperatures/pressure etc.

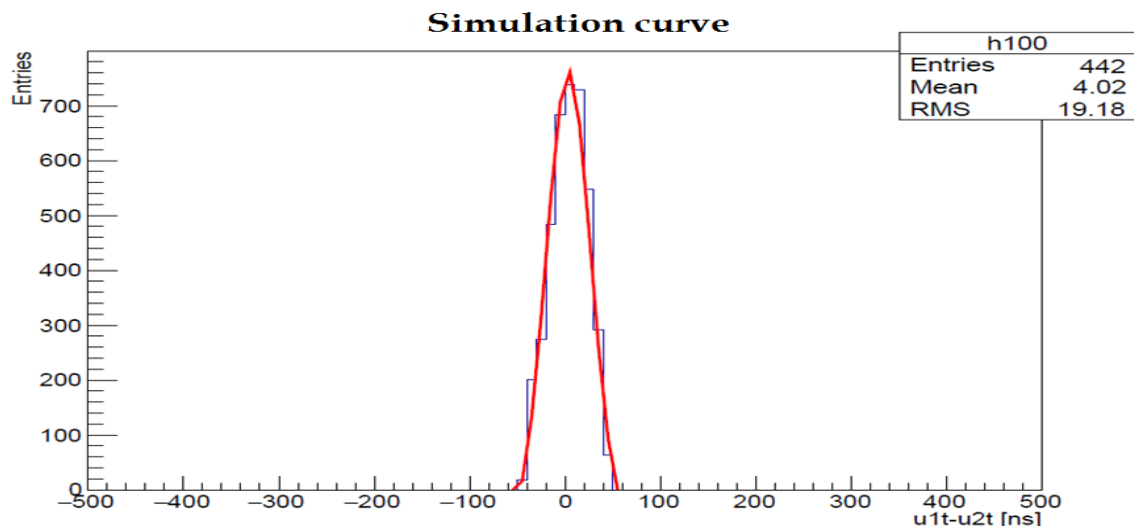


Figure 2.17: Example of a simulation curve

2.6 Detector efficiency

In order to find out the detector efficiency, we got into the study of the V layers: $v1$ and $v2$.

In fact, simply studying U layers, we would not be able to really test our detector.

2.6.1 Comparison between simulation and real data with 4 layers

The first point we have to consider to evaluate detector efficiency is that we should have data in all our layers; as well as we can see in Figure 2.18, data quality looks good and we have data in all devices.

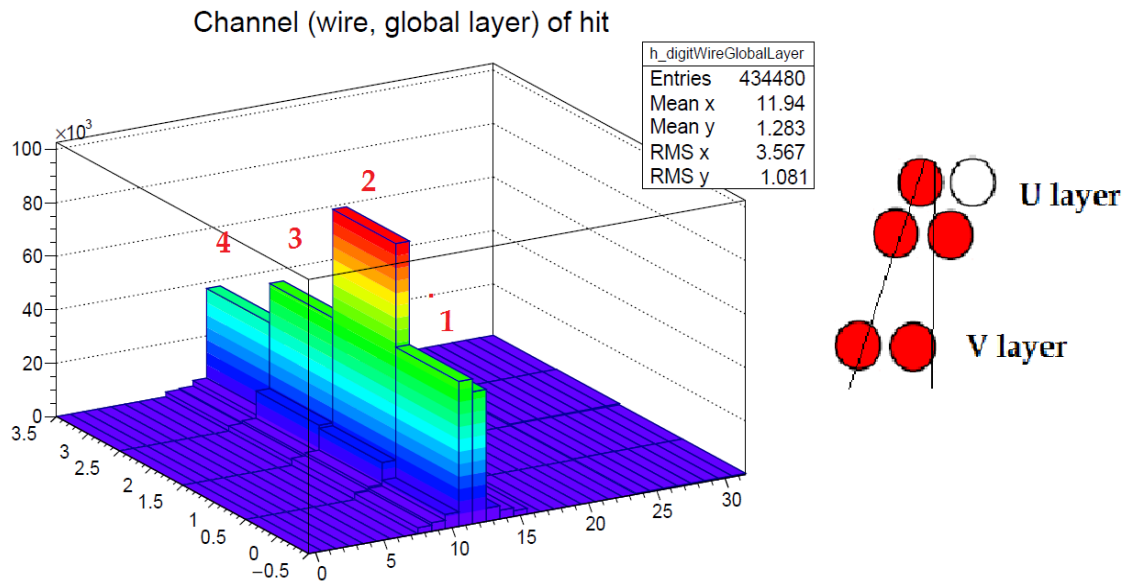


Figure 2.18: Look at test beam data considering 4 layers

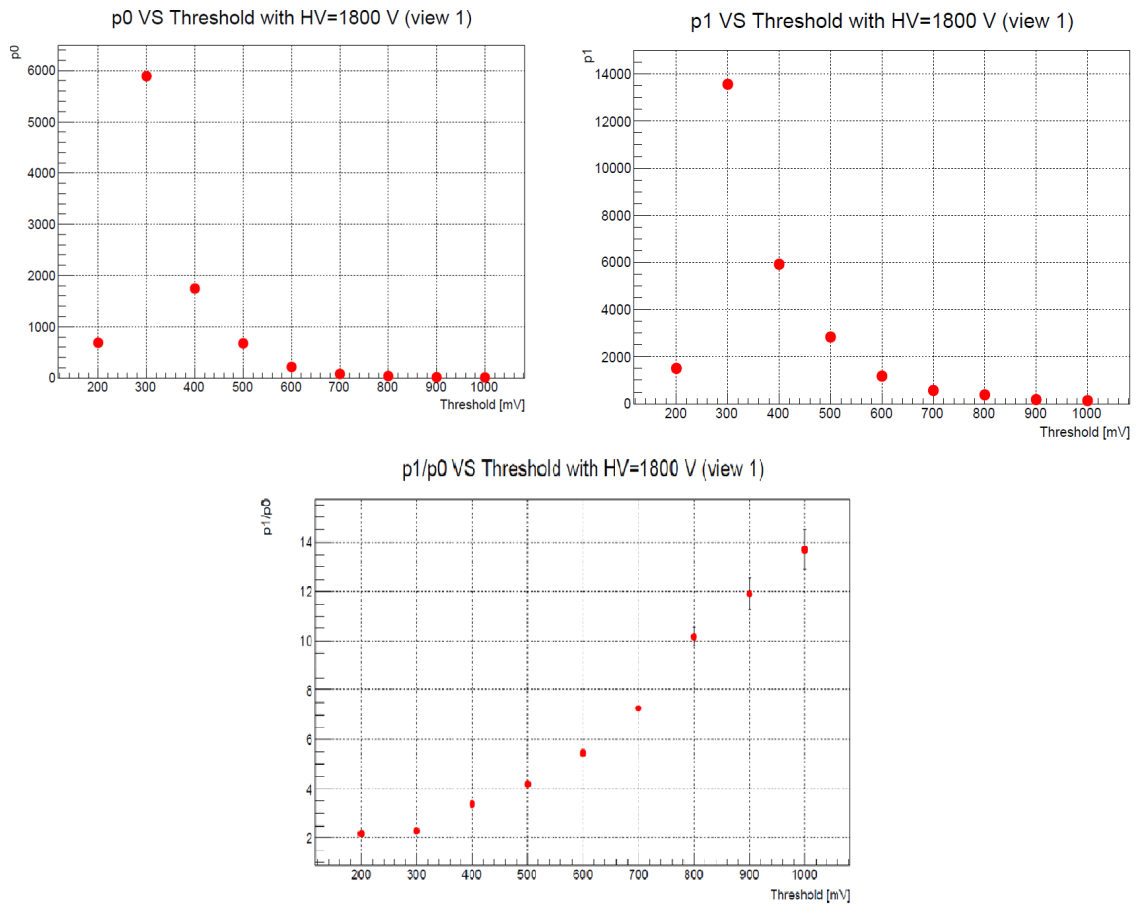


Figure 2.19: ArEt HV = 1800 V p_0 , p_1 and p_1/p_0

We are looking for a cut-threshold or a cut-value that could divide our signal from the noise; we can extrapolate these values because, as shown in Figure 2.19, we have three well-defined signals.

The plot on the bottom, $p1/p0$ plot, looks really good because its meaning is that we are killing more noise than signal.

We want to estimate the efficiency of the detector considering 4 straws; this goal is reached looking at time differences between U layers and V layers.

The value that is estimated through the simulation is $\frac{p1v}{p1u} \approx 1.47$ where $p1v$ is the fit parameter which is extrapolated by the difference between $u1$ layer and $v2$ layer and $p1u$ is the fit parameter which is extrapolated by the difference between $u1$ layer and $u2$ layer. We should underline that the fact that the efficiency is greater than 1 is not a mistake, but it is due to the multiple occupancy of the layers⁴.

As well as you can see from Figure 2.20, this value is higher than every data parameter: there is something wrong with the layers.

In order to understand this unexpected behavior, we have to consider two different configurations with 3 layers, which alternatively include $v1$ layer and $v2$ layer.

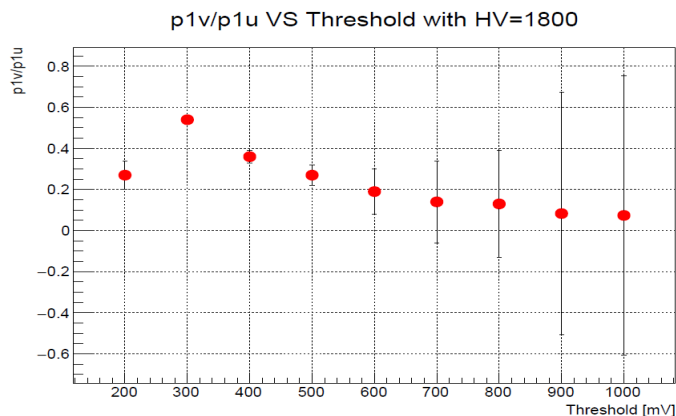


Figure 2.20: *ArEt* HV = 1800 V estimation of efficiency

2.6.2 Comparison between simulation and real data with just 3 layers

This comparison is done between *ArEt* and *ArCO2* mixtures and between two different configurations that are:



Figure 2.21: Layers configurations

⁴the simulation was set in order to include this phenomenon

Efficiency calculated with the ratio between $(u1t - u2t)/(u1t - v1t)$

Looking at Figure 2.22, we should underline some results:

- *ArCO2* efficiency is much higher than *ArEt* one; *ArCO2* signal is bigger than *ArEt* one; this feature represents an unexpected behavior and it should be investigated more deeply;
- the fact that the efficiency is greater than 1 is not a mistake, but it is due to the multiple occupancy of the layers;
- it is good that in *ArEt* ratio plot efficiency decreases with increasing thresholds;
- the fact that *ArCO2* efficiency is almost constant is probably due to the almost constant number of entries we have with every threshold.

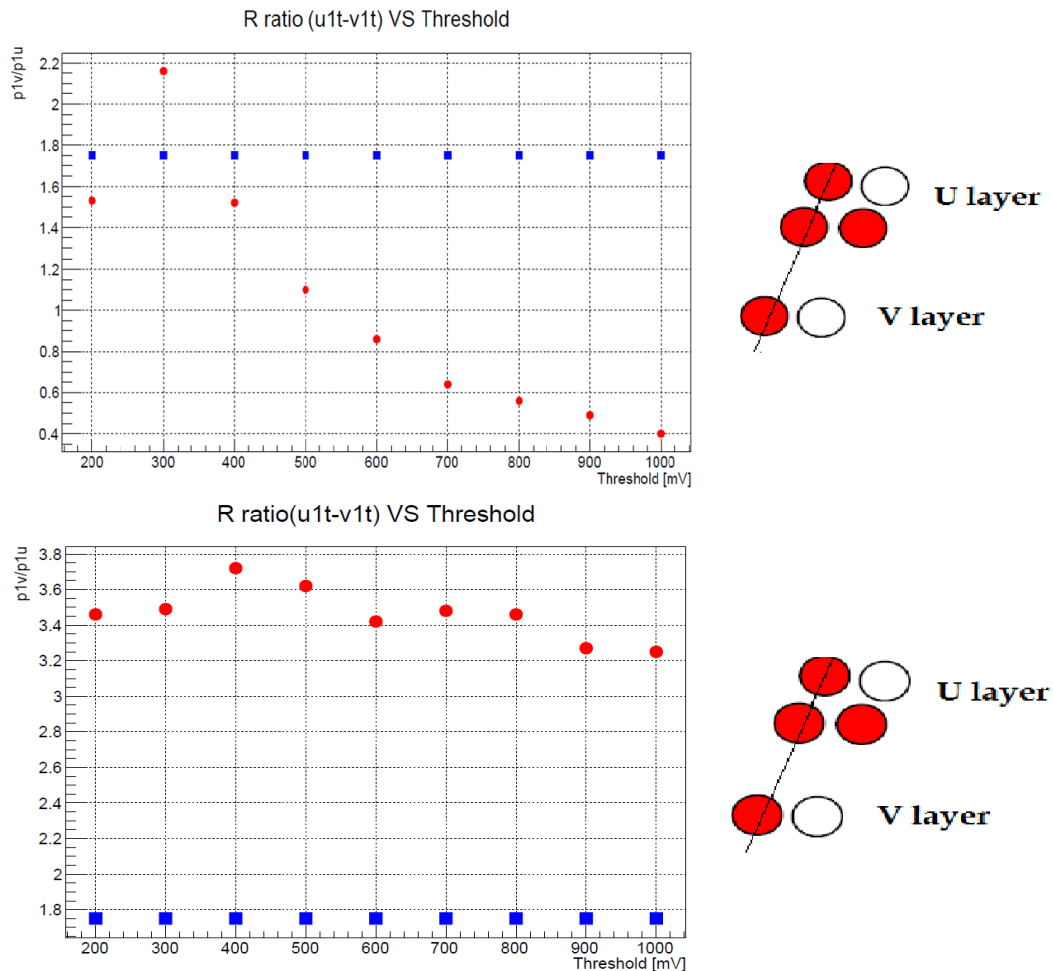


Figure 2.22: On the top: *ArEt* $HV = 1800 V$; on the bottom: *ArCO2* $HV = 1500 V$; in red: test beam data; in blue: simulation

Efficiency calculated with the ratio between $(u1t - u2t)/(u1t - v2t)$

Looking at Figure 2.23, we should underline some results:

- *ArCO2* efficiency is almost equal to *ArEt* one;
- we really don't understand why the efficiencies are so bad → there should be something wrong with *V* layers.

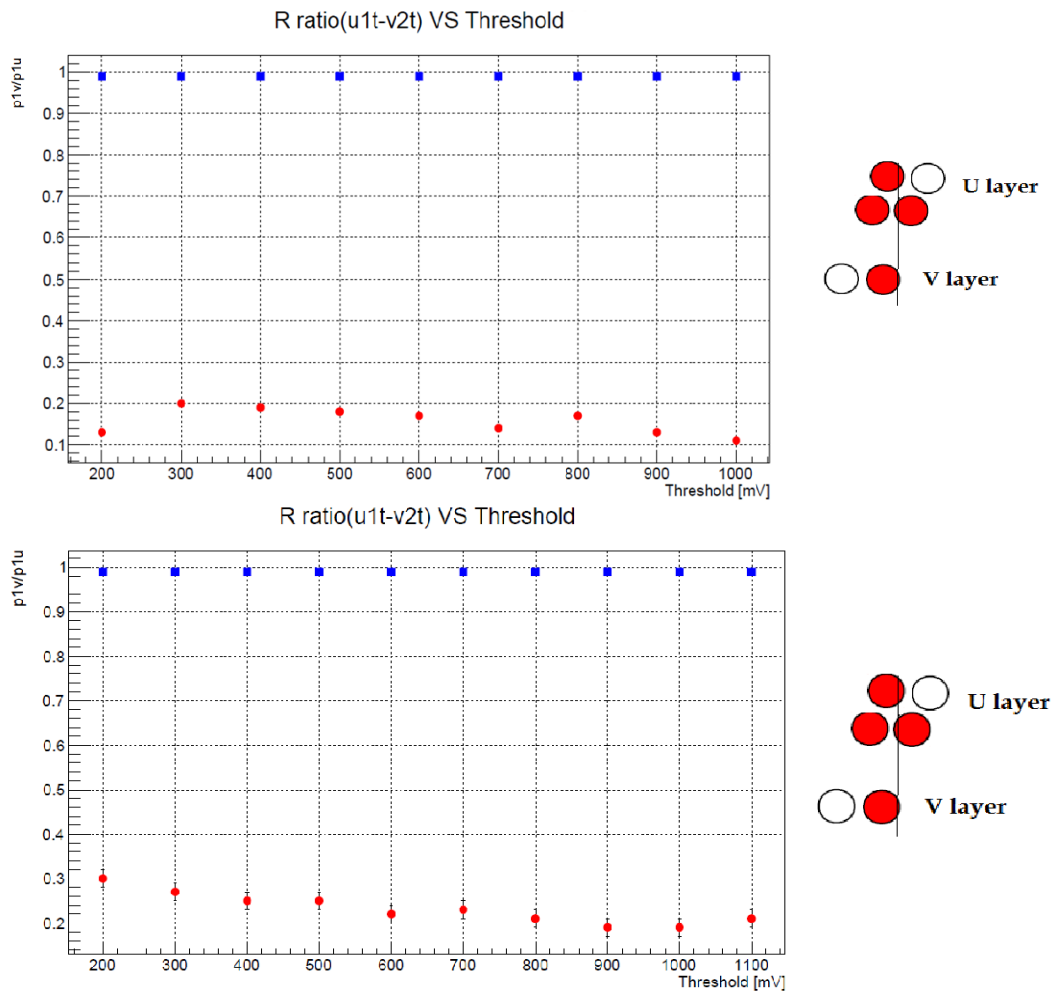


Figure 2.23: On the top: *ArEt* $HV = 1800 V$; on the bottom: *ArCO2* $HV = 1500 V$ estimation of efficiency; in red: test beam data; in blue: simulation

Conclusion

In order to conclude my report, I should draw the necessary conclusions from my work. The most important purpose of my work was to characterize the performance of the tracker detector testing two different gas mixtures, *ArCO2* and *ArEt*.

Using measurement taken with two different sources, ^{90}Sr and ^{55}Fe , I studied the plateau curves and the S/N ratio .

For *ArCO2* (Figure 2.2), it is possible to see a breaking down point in the plateau curve which constitutes a validation of *ArCO2* features: after this point we couldn't count anymore. Regarding *ArEt*, in Figure 2.3, I observed an unexpected behavior: there is no turn over at all.

For *ArCO2*, the S/N ratio is higher than 7 : 1; ideally this ratio should be like 10 : 1, so the estimated value looks pretty good.

ArEt was tested both in the vacuum chamber and outside of it. Unlike *ArCO2*, it seemed that this gas mixture was not working really well. In fact, some data looked really bad and we couldn't understand the measurements we were taking. Although it is good that the ratios outside and in the vacuum chamber were comparable, I obtained ratios that were about 3 : 1: they were supposed to be better and they were supposed to be 10 times that of *ArCO2* so there is something wrong we didn't understand.

The characterization of the performance of the detector went on with test beam data taken from the 120 GeV proton beam.

I looked for a cut-threshold or a cut-value that could divide our signal from the noise; these values were taken fitting our signal with a gaussian and a flat fit.

In order to reduce background, I estimated a possible cross-talk between capacitors. Since the ratios which are related to the cross-talk are almost constant, within their uncertainty, it is possible to conclude that, despite of a high occupancy in the beam, there is no real indication or evidence of cross-talk.

Finally I wanted to estimate the efficiency of the detector considering 4 layers; this goal was reached looking at time differences between U layers and V layers.

Since the efficiency calculated considering 4 layers was bad, I analysed two different configurations of 3 layers. These are the results I obtained with one configuration (Figure 2.22):

- *ArCO2* efficiency is much higher than *ArEt* one; *ArCO2* signal is bigger than *ArEt* one; this feature represents an unexpected behavior and it should be investigated more;
- the fact that the efficiency is greater than 1 is not a mistake, but it is due to the multiple occupancy of the layers;

- it is good that in $ArEt$ ratio plot efficiency decreases with increasing thresholds;
- the fact that $ArCO2$ efficiency is almost constant is probably due to the almost constant number of entries I have with every threshold.

Results obtained with the other configuration (Figure 2.23):

- $ArCO2$ efficiency is almost equal to $ArEt$ one;
- we really don't understand why the efficiencies are so bad → there should be something wrong with V layers.

Bibliography

- [1] *Muon g-2 Technical Design Report*, June 2015;
- [2] David W. Hertzog: *A new muon g-2 experiment at Fermilab: why, when and how*, May 2011;
- [3] Joseph Grange: *The New Muon g-2 Experiment at Fermilab*, January 2015 ;
- [4] Graziano Venanzoni: *The New Muon g-2 experiment at Fermilab*, November 2014;
- [5] Walter H. Toki: *Review of Straw Chambers*, March 1990;
- [6] F. Sauli: *Principles of operation of Multiwire Proportional and Drift Chambers*, 1975-1976 ;
- [7] Dan Gastler: *Tracker Electronics Status*, December 2013;
- [8] Tom Stuttard: *Tracker test beam analysis update*, September 2015;
- [9] Becky Chislett: *Tracker Related Physics Studies* , March 2015;